

## 2018 EMP Zooplankton Summary Report

### Introduction:

Zooplankton sampling has been conducted since 1974 at least once a month at 20 fixed stations in the upper SFE (Figure 1). Three gear types are used for each sampling event: a pump with a 43-micron mesh net for micro-zooplankton (rotifers, nauplii, and small cyclopoid copepods); a Clarke-Bumpus (CB) net with a 160-micron mesh for sampling meso-zooplankton (cladocerans and most juvenile and adult calanoid copepods); and a mysid net with a 505-micron mesh for sampling mysid shrimp and other macro-zooplankton. Both the mysid and CB nets are attached to a sled and towed obliquely from the bottom through the surface for a 10-minute tow. Volume is measured using a General Oceanics flowmeter placed in the mouth of each net so that:  $V = (end\ meter - start\ meter) * k * a$ ; where  $V$  is the volume of water sampled,  $k$  is a flowmeter correction value, and  $a$  is the area of the mouth of the net. The Teel Marine 12V utility pump is also used at each station to sample approximately 19.8 gallons from the entire water column, which is filtered through a 43-micron mesh net to concentrate the sample. Samples are preserved in 10% formalin with Rose Bengal dye before being processed in the laboratory for identification and enumeration of organisms using either a microscope. More information about the sampling and processing methods can be found in the metadata at [ftp://ftp.wildlife.ca.gov/IEP\\_Zooplankton/](ftp://ftp.wildlife.ca.gov/IEP_Zooplankton/).

Abundance indices are calculated for each organism based on the gear type most effective at its capture and reported as the mean catch-per-unit-effort (CPUE). CPUE is calculated as the number of each organism collected per cubic meter of water sampled, so that:  $CPUE = s * V^{-1}$ ; where  $s$  is the estimated count of the target organism in the sample. Copepod abundance indices reported here only include adults, as juveniles were not always accurately identified to species. Annual and seasonal abundance indices were calculated using 14 fixed stations sampled consistently since 1974 (Figure 1) and 2 non-fixed stations sampled where bottom specific conductance was roughly 2 and 6 millisiemens per centimeter (approximately 1 and 3 psu).

To analyze long-term trends (1974 to present), annual abundance indices were calculated as the mean CPUE for samples collected from March through November, as winter sampling was inconsistent before 1995. Seasonal abundance indices were calculated as the mean CPUE for samples collected during each season: winter (previous December to February), spring (March to May), summer (June to August), and fall (September to November). Long-term seasonal trends for winter are only shown for 1995 to present.

Spatial distribution indices for organisms is described as seasonal mean CPUE for by region. Estuary regions were defined as San Pablo Bay (stations D41 and D41A), Suisun Bay (stations D6, 28, 54, and 48), Suisun Marsh (stations 32 and S42), West Delta (stations 60, 64, and 74), Central Delta (stations D16, 86, and D28), and the East Delta (92 and M10).

Overall abundance of almost all zooplankton in the estuary, especially native species, has dropped significantly since 1974 (Figure 2). Only the abundance of cyclopoid copepods increased in the estuary in this period, driven by the invasion and spread of *Limnoithona tetraspina*. The overall decrease in zooplankton abundance in the estuary can be attributed to a series of invasions into the estuary, most notably that of the Asian clam *Potamocorbula amurensis* in the mid-1980s (Kimmerer, Gartside, and Orsi 1994; Carlton et al. 1990). *P. amurensis* spread throughout the SFE and within 2 years of its introduction had disastrous impacts on the planktonic community of the upper estuary due to its high filtration feeding rates on phytoplankton and copepod nauplii.

#### **Calanoida:**

While overall calanoid copepod abundance has declined slightly over the study period, community composition has shifted dramatically (Figure 2A). The copepods *Eurytemora affinis* and *Acartia* spp. dominated the calanoid community when the study began. The non-native *E. affinis* was once the primary prey item of the endangered Delta Smelt, but its abundance has declined to a fraction of what it once was, forcing fish to prey switch to recently introduced non-native calanoids (Moyle et al. 1992; Slater and Baxter 2014). One of the first recorded introduced calanoid copepods was *Sinocalanus doerrii*, a freshwater species native to China that invaded the estuary in 1978 and became the most dominant calanoid species in the estuary for a decade (Orsi et al. 1983). Then in 1987, after the invasion of *P. amurensis*, the calanoid copepod *Pseudodiaptomus forbesi* was introduced to the system, which competed with *E. affinis* and further changed SFE's calanoid community (Orsi and Walter 1991). *P. forbesi* quickly became the numerically dominant calanoid copepod in the upper estuary as other species declined in abundance. Another invasion occurred in 1993, when the predatory calanoid *Acartiella sinensis* quickly became the second most abundant calanoid in the upper estuary, dominating the low-salinity zone (Orsi and Ohtsuka 1999). This invasion is hypothesized to have narrowed the range of *P. forbesi* towards the freshwater zone of the estuary, as predation on *P. forbesi* nauplii by *A. sinensis* has been recorded (Kayfetz and Kimmerer 2017). In general, calanoid copepod abundance is highest in the estuary during the summer and fall months, with lower abundance during winter.

While calanoid copepod abundance peaked in the summer of 2017 at a nearly 20 year high, 2018 abundance returned to levels comparable to the previous two decades (Figure 3A). The 2017 peak was driven by increases in the abundance of *Pseudodiaptomus forbesi* during summer (Figures 2A, 3A) in the Suisun region (Hennessy 2018). This 2017 peak corresponds with record precipitation levels and Delta outflows, which caused the low salinity zone to extend throughout Suisun well into the warm summer months. This contrasts with 2018, a lower outflow year, when *P. forbesi* abundance was lower, and distribution of the species shifted eastward into the Delta. The correlation between summer outflows and zooplankton abundances has also been witnessed amongst *Synchaeta* spp. of rotifers in 2017, and mysid species before the invasion of *P. amurensis*.

In 2018 the predatory *Acartiella sinensis* was seen in highest densities in the summer and fall and was found mostly in the Suisun and West Delta regions, similar to the prior year. In fall 2018, *A. sinensis* was the most abundant calanoid in Suisun and the West Delta, where it co-occurred with high densities of one of its prey items *Limnoithona tetraspina* (Figure 4B), while *P. forbesi* shifted eastward from Suisun (Figure 4A). *Eurytemora affinis*, once the most abundant copepod in the estuary, peaked in abundance in the spring of 2018 in Suisun Marsh, with occurrences also further upstream in the Delta. This was different than its 2017 distribution, when it was restricted to Suisun Marsh and downstream during the spring, likely also tied to high outflow in the system (Hennessy 2018). *Acartia* spp. was the only native calanoid copepod found common in 2018, mostly restricted to the higher-salinity region of San Pablo Bay during the winter.

### **Cyclopoida:**

While calanoid abundance declined and the community composition dramatically changed, the abundance of cyclopoid copepods exploded since the study first began (Figure 2B). The native *Oithona* spp. and *Acanthocyclops* copepods were at low abundances when the study began, but with the introduction of *Limnoithona sinensis* in the early 1980s, and the later identification of the invasive *Limnoithona tetraspina* in 1993, cyclopoid indices have increased dramatically (Ferrari and Orsi, 1984; Orsi and Ohtsuka, 1999). Abundance indices for the two species of *Limnoithona* were reported together from 1980 through 2006 as *Limnoithona* spp., then separately since 2007 when they were identified and enumerated separately as *L. sinensis* and *L. tetraspina*. Much smaller than calanoid copepods collected in the CB net, the *Limnoithona* cyclopoids are best retained in pump samples, which use a smaller mesh. Since the early 1990s, *Limnoithona* spp. abundance has been higher than calanoid copepod abundance, and the small *L. tetraspina* has become the most common copepod in the upper estuary. This increase *L.*

*tetraspina* abundance is likely due to a decline of Northern Anchovy in the upper SFE and subsequent decreased predation, as well as the cyclopoid's small size and motionless behavior, making it very difficult for visual feeders to capture (Bouley and Kimmerer 2006; Greene et al. 2011). The introduction of *L. tetraspina* is also linked to the reduction of the range of *P. forbesi* out of the low-salinity zone of the estuary, as high *L. tetraspina* densities may have fed and sustained larger populations of the predatory *A. sinensis*, which also fed on *P. forbesi* nauplii (Kayfetz and Kimmerer 2017). Seasonally, *L. tetraspina* peaks in summer and fall (Figure 3B), with lower abundance in winter and spring, and in 2018 *L. tetraspina* abundance was the highest observed for all copepods.

In 2018 *Limnoithona tetraspina* was once again the most abundant copepod in the estuary, as it has been since 1994. As in prior years, this cyclopoid was most abundant in the low-salinity zone of the estuary in Suisun and the West Delta, with lower abundances during winter and spring, before its population increased and peaked in summer and fall (Figure 4B). *Oithona davisae*, a native cyclopoid, was the most abundant cyclopoid in the higher-salinity San Pablo Bay through the year, with population peaks in summer and fall (Figure 4B). The numerical dominance of *L. tetraspina* in the low-salinity zone, a region where other copepods have declined with the introduction of *Potamocorbula amurensis* could be due to the cyclopoids smaller size, high growth rates, and relatively motionless behavior (Bouley and Kimmerer 2006). These characteristics may make it more able to escape predation in a region where visual predation is most dominant among fish (Kimmerer 2006).

#### **Cladocera:**

The cladoceran community of the upper estuary is composed of *Bosmina*, *Daphnia*, *Ceriodaphnia*, and *Diaphanosoma* species, whose populations have also significantly declined since the onset of the study (Figure 2C). These cladocera tend to be herbivorous, feeding primarily on phytoplankton, and were likely hard hit by the invasion of *P. amurensis* (Baxter et al. 2008; Kratina and Winder 2015). Cladocerans make up a significant portion in the diets of Delta Smelt, juvenile Chinook Salmon, and young-of-the-year Striped Bass throughout the upper estuary (Heubach et al. 1963; Slater and Baxter 2014; Goertler et al. 2018). While Cladocera abundance has declined, in recent years summer abundance has been increasing and in 2018, summer cladocera abundance was the highest observed since the *P. amurensis* invasion (Figure 3C). The invasion and increase of available copepod prey such as *P. forbesi* has created a shift in the nutritional content of the plankton community away from Cladocera, which could have had benefits and drawbacks for fish in the region (Kratina and Winder 2015).

Cladocera abundance was at a 10-year high in 2018 (Figure 2C), but still low compared to historical numbers. While in 2017 some cladocera, namely *Bosmina*, were found down-river in Suisun and the West Delta, in 2018 the highest densities of cladocera were found in the East Delta, with trace concentrations found in other regions of the estuary, and abundance peaked in summer (Figure 4C).

#### **Rotifer:**

While they are the most abundant zooplankton in the estuary, long-term sampling of rotifers using the pump system shows a dramatic decrease in their annual abundance in the estuary since the beginning of this study (Figure 2D). Several species of rotifers that make up the community; most abundant are the *Polyarthra*, *Synchaeta*, and *Keratella* genera. Interestingly, the decline of rotifer abundance beginning in the late 1970s preceded the invasion of *P. amurensis* in the estuary (Cloern and Jassby 2012). In 2018, rotifer abundance was as low as the last two decades, whereas in 2017, a record high outflow year, had the highest abundance in nearly 30 years (Figure 2D). *Keratella* and *Polyarthra* tend to be most abundant in the fresh-water and low-salinity zone of the estuary, while *Synchaeta* species occur most in the higher-salinity areas of San Pablo Bay and Suisun (Figure 4D)(Winder and Jassby 2011).

Rotifers were the most abundant zooplankton sampled during 2018 and were found throughout the estuary (Figure 4D). A spatial and temporal split was discernable between *Synchaeta* and other rotifers, with *Synchaeta* having highest densities in San Pablo Bay during the spring, and other rotifers being most abundant in the East Delta in summer. The distribution and abundance of rotifers differed significantly between 2017 and 2018, as 2017 rotifer abundances were double those of 2018, and *Synchaeta* peaked in Suisun Marsh in 2017 (Hennessy 2018).

#### **Mysida:**

Not only have mysid abundances declined significantly since the 1970s, but the community has also shifted from being composed almost entirely by the native *Neomysis mercedis*, to being dominated by the non-native *Hypercanthomysis longirostris* (formerly *Acanthomysis bowmani*) (Figure 2E). The first significant decline in *N. mercedis* occurred during the 1976-1977 drought, likely caused by food limitation from an absence of diatoms due to very low river discharges (Siegfried et al. 1979; Cloern et al. 1983). The populations of *N. mercedis* were able to rebound after the years of drought and stayed at high densities in the Suisun Bay region of the upper estuary until the introduction of *P. amurensis* in the mid-1980s, after which their numbers crashed. In 1993 the introduced *H. longirostris* was first detected by this study, shortly after the decline of *N. mercedis*, and it quickly became the most common mysid in the system. However, overall mysid abundances have not returned to their pre-clam invasion levels

(Modlin and Orsi 1997, Figure 2E). Mysids have always peaked in the spring and summer months, fluctuating with the higher productivity in the estuary during those seasons (Figure 3E). Historically mysids have been of critical importance in the diets of many fish species in the SFE including Delta Smelt, Longfin Smelt, Striped Bass, and Chinook Salmon (Moyle et al. 1992; Feyrer et al. 2003; CDFG 2009; Goertler et al. 2018). However, the decline of mysids in the upper estuary has resulted in a significant decrease in their presence in the diets of fishes of the region (Feyrer et al. 2003).

This general decline in abundance continued in 2018, even though 2017 saw a peak in mysid abundances (Figure 2E), and the distribution and timing of peaks has stayed similar over the last two decades (Figure 4E; Hennessy 2018). *Hyperacanthomysis longirostris* was again the most common mysid in the estuary during all seasons, while the once common and native *Neomysis mercedis* continued to be almost imperceptible in the region. This has been the overall trend in the estuary's mysid communities since 1994. As in prior years, mysids in 2018 were most abundant during the summer, and highest concentrations occurred in the low-salinity zone of Suisun Bay and Marsh and the West Delta.

## References:

- Baxter R, Feyrer F, Nobriga M, Sommer T. 2008. Pelagic Organism Decline Progress Report: 2007 Synthesis of Results.
- Bouley P, Kimmerer WJ. 2006. Ecology of a highly abundant, introduced cyclopoid copepod in a temperate estuary. *Mar Ecol Prog Ser.* 324(October):219–228.
- Carlton JT, Thompson JK, Schemel LE, Nichols FH. 1990. Remarkable invasion of San Francisco Bay (California, USA) by the Asian clam *Potamocorbula amurensis*. I. Introduction and dispersal. *Mar Ecol Prog Ser.* 66:81–94.
- CDFG. 2009. A Status Review of the Longfin Smelt (*Spirinchus thaleichthys*) in California. Sacramento.
- Cloern JE, Alpine AE, Cole BE, Wong RLJ, Arthur JF, Ball MD. 1983. River discharge controls phytoplankton dynamics in the northern San Francisco Bay estuary. *Estuar Coast Shelf Sci.* 16(4):415–429.
- Cloern JE, Jassby AD. 2012. Drivers of change in estuarine-coastal ecosystems: Discoveries from four decades of study in San Francisco Bay. *Rev Geophys.* 50:4001.
- Ferrari FD, Orsi J. 1984. *Oithona davisae*, New Species, and *Limnoithona sinensis* (Burckhardt, 1912) (Copepoda: Oithonidae) from the Sacramento-San Joaquin Estuary, California. *J Crustac Biol.* 4(1):106–126.
- Feyrer F, Herbold B, Matern SA, Moyle PB. 2003. Dietary shifts in a stressed fish assemblage: Consequences of a bivalve invasion in the San Francisco Estuary.
- Goertler P, Jones K, Cordell J, Schreier B, Sommer T. 2018. Effects of extreme hydrologic regimes on juvenile Chinook Salmon prey resources and diet composition in a large river floodplain. *Trans Am Fish*

Soc. 147:287–299.

Greene VE, Sullivan LJ, Thompson JK, Kimmerer WJ. 2011. Grazing impact of the invasive clam *Corbula amurensis* on the microplankton assemblage of the northern San Francisco estuary. *Mar Ecol Prog Ser.* 431(February):183–193.

Hennessy A. 2018. Zooplankton Monitoring 2017. *Interag Ecol Progr Newsl.* 32(1):21–32.

Heubach W, Toth RJ, Mccready AM. 1963. Food of Young-of-the-year Striped Bass (*Roccus Saxatilis*) in the Sacramento-San Joaquin River. *Calif Fish Game.* 49(4):224–239.

Kayfetz K, Kimmerer W. 2017. Abiotic and biotic controls on the copepod *Pseudodiaptomus forbesi* in the upper San Francisco Estuary. *Mar Ecol Prog Ser.* 581(Runge 1988):85–101.

Kimmerer WJ. 2006. Response of Anchovies dampens effects of the invasive bivalve *Corbula amurensis* on the San Francisco Estuary foodweb. *Mar Ecol Prog Ser.* 324:207–218.

Kimmerer WJ, Gartside E, Orsi JJ. 1994. Predation by an introduced clam as the likely cause of substantial declines in zooplankton of San Francisco Bay. *Mar Ecol Prog Ser.* 113(1–2):81–94.

Kratina P, Winder M. 2015. Biotic invasions can alter nutritional composition of zooplankton communities. *Oikos.* 124:1337–1345.

Modlin RF, Orsi JJ. 1997. *Acanthomysis bowmani*, a new species, and *A. aspera* li, Mysidacea newly reported from the Sacramento-San Joaquin Estuary, California (Crustacea: Mysidae). *Proc Biol Soc Washingt.* 110(3):439–446.

Moyle PB, Herbold B, Stevens DE, Miller LW. 1992. Life history and status of delta smelt in the Sacramento-San Joaquin estuary, California. *Trans Am Fish Soc.* 121(1):67–77.

Orsi J, Walter TC. 1991. *Pseudodiaptomus forbesi* and *P. marinus* (Copepoda: Calanoida), the latest copepod immigrants to California's Sacramento-San Joaquin Estuary. *Bull Plankt Soc Japan.*:553–562.

Orsi JJ, Bowman TE, Marelli DC, Hutchinson A. 1983. Recent introduction of the planktonic calanoid copepod *Sinocalanus doerrii* (Centropagidae) from mainland China to the Sacramento-San Joaquin Estuary of California. *J Plankton Res.* 5(3):357–375.

Orsi J J, Ohtsuka S. 1999. Introduction of the Asian copepods *Acartiella sinensis*, *Tortanus dextrilobatus* (Copepoda: Calanoida), and *Limnoithona tetraspina* (Copepoda: Cyclopoida) to the San Francisco Estuary, California, USA. *Plankt Biol Ecol.* 46(2):128–131.

Orsi James J., Ohtsuka S. 1999. Introduction of the Asian copepods *Acartiella sinensis*, *Tortanus dextrilobatus* (Copepoda : Calanoida), and *Limnoithona tetraspina* (Copepoda : Cyclopoida) to the San Francisco Estuary, California, uSA. *Plankt Biol Ecol.* 46(2):128–131.

Siegfried CA, Kopache ME, Knight AW. 1979. The Distribution and Abundance of *Neomysis mercedis* in Relation to the Entrapment Zone in the Western Sacramento-San Joaquin Delta. *Trans Am Fish Soc.* 108(3):262–270.

Slater SB, Baxter R. 2014. Diet, Prey Selection, and Body Condition of Age-0 Delta Smelt, *Hypomesus transpacificus*, in the Upper San Francisco Estuary. *San Fr Estuary Watershed Sci.* 12(3):1–24.

Winder M, Jassby AD. 2011. Shifts in Zooplankton Community Structure: Implications for Food Web Processes in the Upper San Francisco Estuary. *Estuaries and Coasts.* 34:675–690.



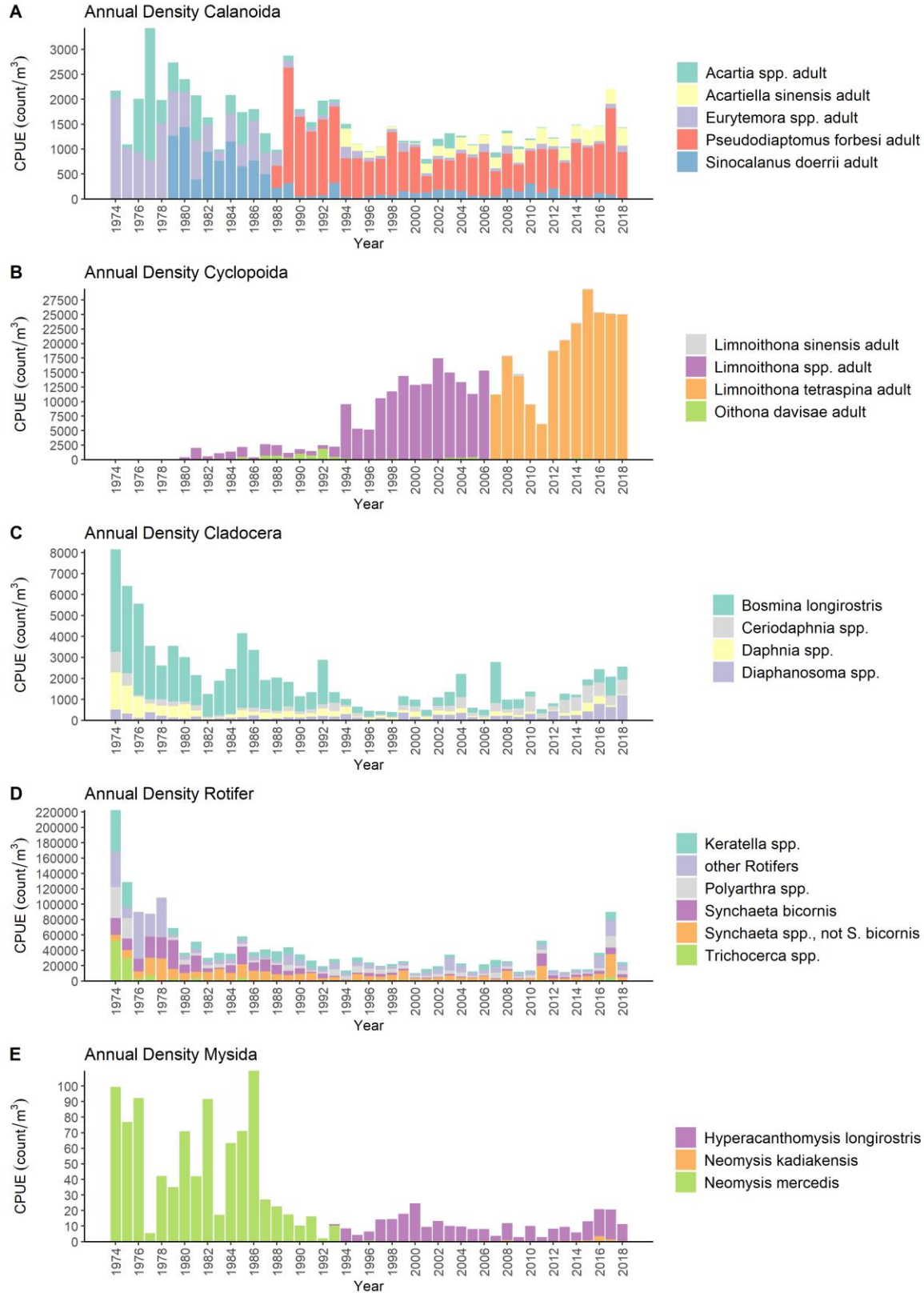


**Figure 2: Annual (Mar-Nov) mean zooplankton CPUE for A) Calanoid CPUE in the CB net, B) Cyclopoida CPUE in pump samples, C) Cladocera CPUE in the CB net, D) Rotifer CPUE in pump samples, and E) Mysid CPUE in the mysid net.**

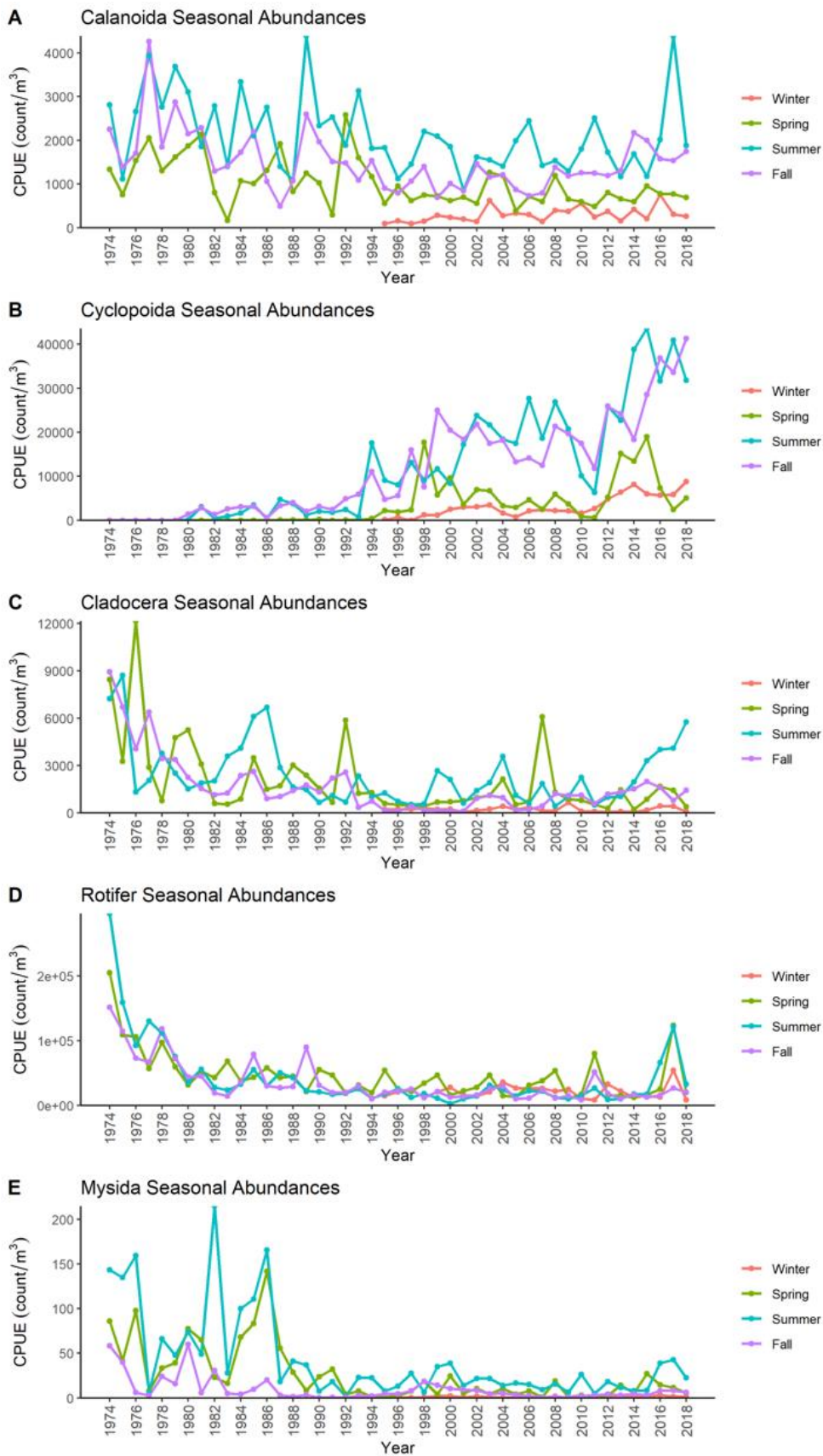
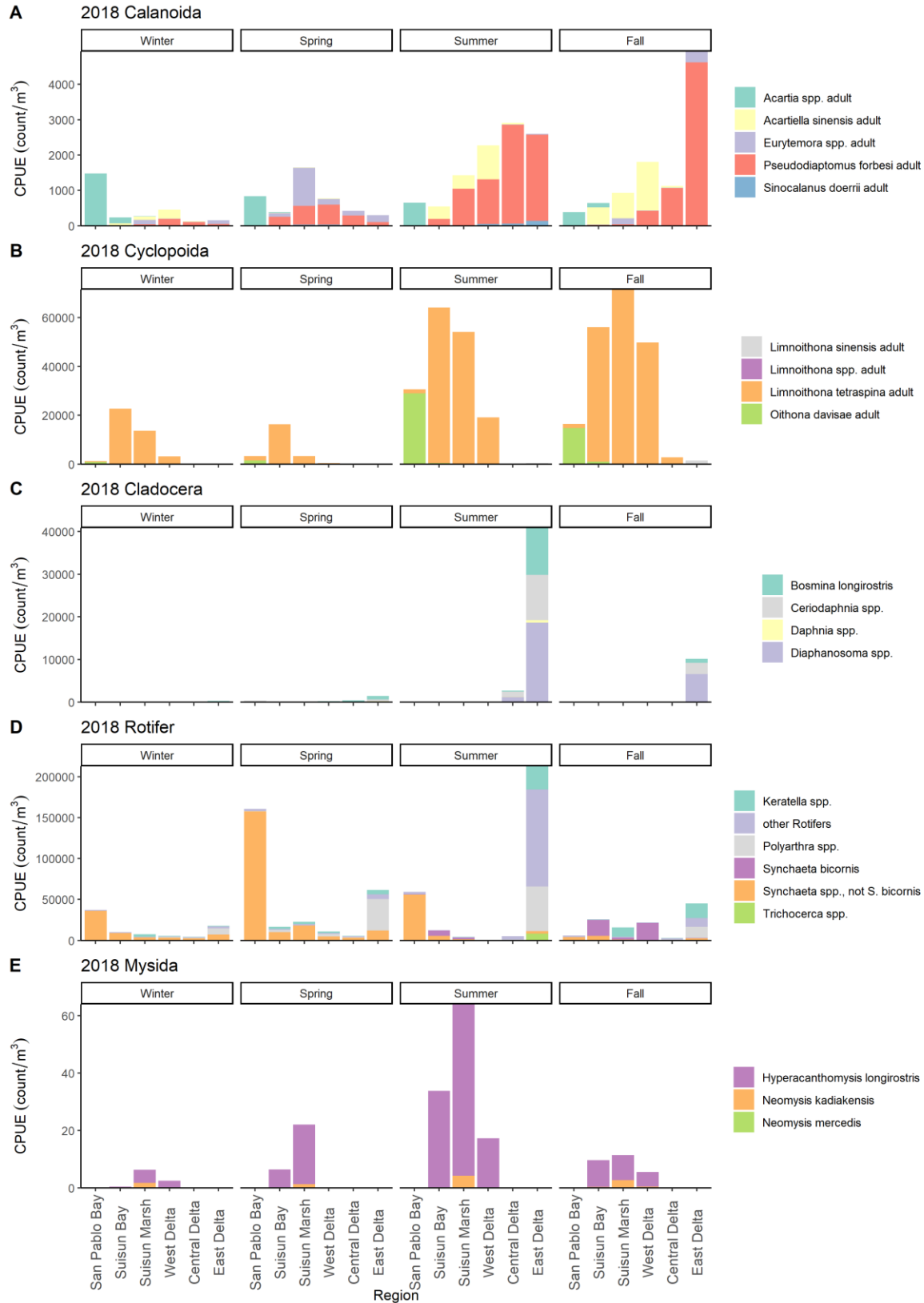


Figure 3: Seasonal mean zooplankton CPUE. Spring, summer, and fall are reported for 1974-2018, winter is reported for 1995-2018. A) Calanoid CPUE in the CB net. B) Cyclopoida CPUE in pump samples. C) Cladocera CPUE in the CB net. D) Rotifer CPUE in pump samples. E) Mysid CPUE in the mysid net.



**Figure 4: Seasonal mean zooplankton CPUE for 2018 by region for A) Calanoid CPUE in the CB net, B) Cyclopoida CPUE in pump samples, C) Cladocera CPUE in the CB net, D) Rotifer CPUE in pump samples, and E) Mysid CPUE in the mysid net.**